Efficiency improvement of an all-vanadium redox flow battery by harvesting low-grade heat

Danick Reynard, C.R. Dennison, Alberto Battistel* and Hubert H. Girault

Ecole Polytechnique Fédérale de Lausanne (EPFL), Laboratoire d'Electrochimie Physique et Analytique (LEPA), Rue de l'Industrie 17, CH-1951 Sion, Switzerland.

**E-mail: alberto.battistel@epfl.ch*

Electronic Supplementary Information

This supplementary information contains:

A. Details of the experimental setup for TREC-VRFB
B. Details of the thermal stability study
C. Arrhenius study of vanadium redox couples
D. Photovoltaic and TREC-VRFB combination

A. Details of the experimental setup for TREC-VRFB

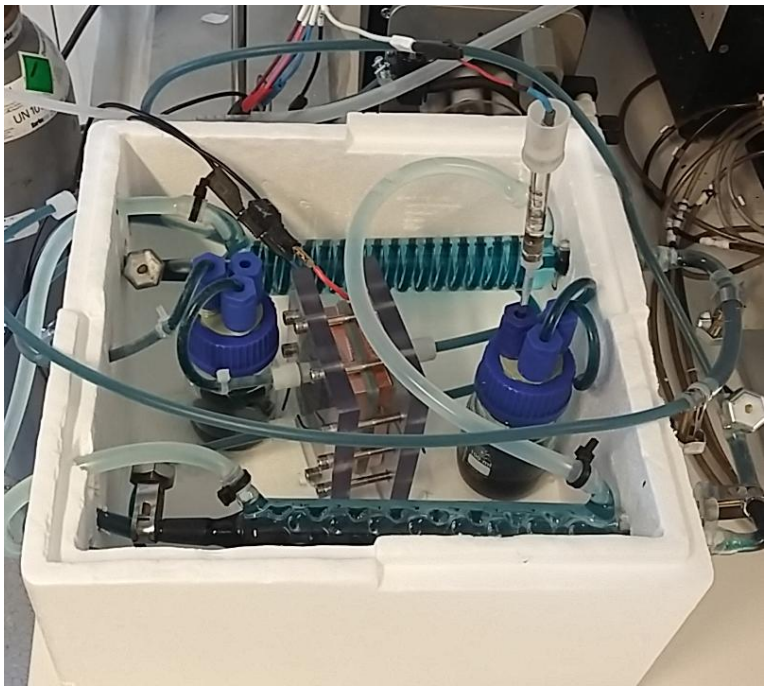

Figure S1: *photo of TREC-VRB experimental setup.*

Figure S1 shows a photo of the experimental setup. A polystyrene box was used for thermal isolation and as retention trail. Cooling and heating liquid circulated in silicon tubes and vanadium electrolyte in PTFE tubes. Two heat exchangers were used. These were made of borosilicate glassware normally used for distillation. The positive electrolyte tanks contained the reference electrode with a long double junction. Having the reference electrode in this tank permitted to monitor better the potential on the positive electrode thus avoiding corrosion.

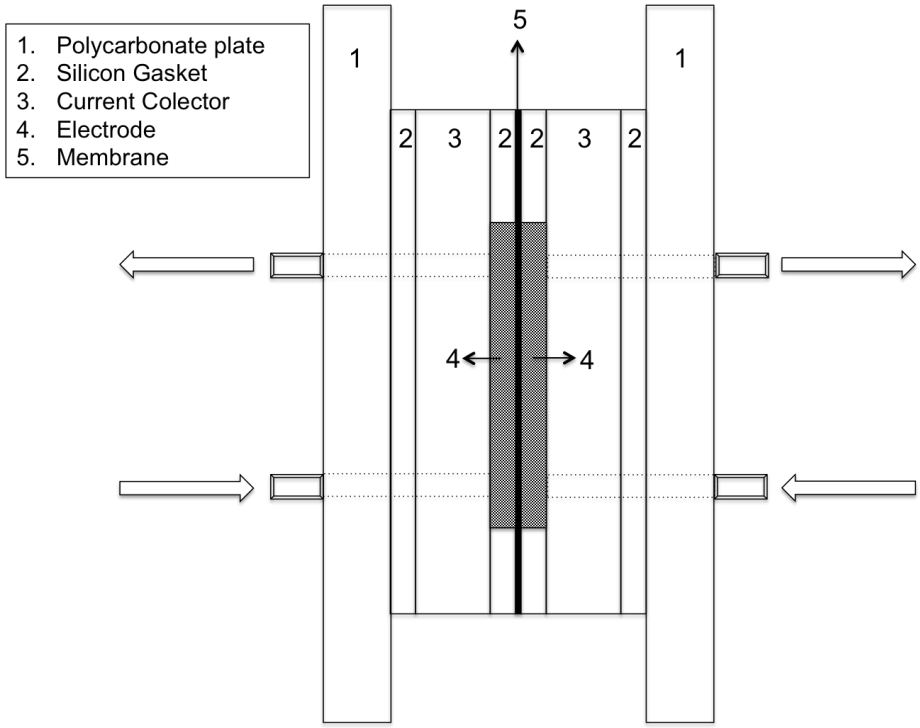

Figure S2: *Schematic representation of the experimental electrochemical cell.*

Schematic of the electrochemical cell is represented in Figure S2. The electrolyte entered the cell from the bottom to help carrying away gas from the cell. The polycarbonate plates assured compression for the cell through screws (not shown). These kept the sealing on the gaskets and improved the electrical contact between the electrode material (carbon felt) and the current collectors. Two screws per current collector were used for electrical lead connections.

B. Details of the thermal stability study

The thermal stability of vanadium redox flow batteries is determined by the stability of V^V species. In fact, at high temperature V^V converts into vanadium pentoxide.

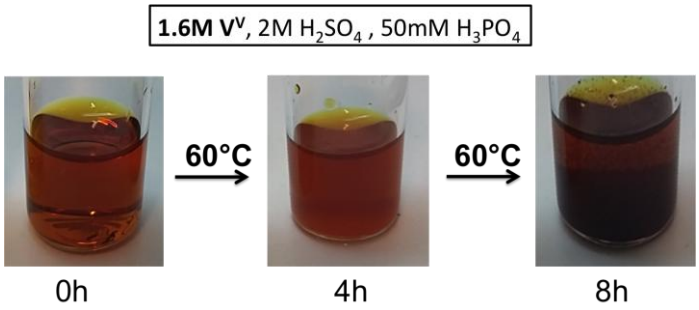

Figure S3: *thermal behavior of commercial electrolyte with 1.6 M V^V at 60 °C.*

Figure S3 shows the behaviour of the *commercial electrolyte* with 1.6 M V^V at 60 °C. The solution was initially dark orange and transparent. After 4 hours, the solution lost its transparence, but there was no clear sign of precipitation on the bottom of the vial. However, after other 4 hours the solution was clearly darker and some precipitated was observable on the bottom.

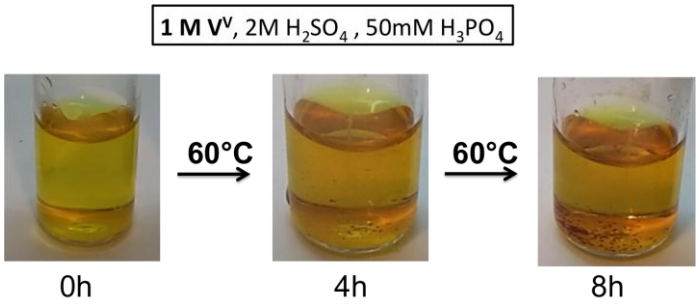

Figure S4: *thermal behavior of commercial electrolyte with 1 M V^V at 60 °C.*

The behaviour was different decreasing the V^V concentration to 1 M (Figure S4). The solution was initially yellow, but some small orange/red particles appeared on the bottom after 4 hours at 60 °C. The amount and size of particles increased after other 4 hours.
Because of these findings, it was decided to allow a maximum time of 4 hours and a maximal temperature of 60 °C for the next experiments.

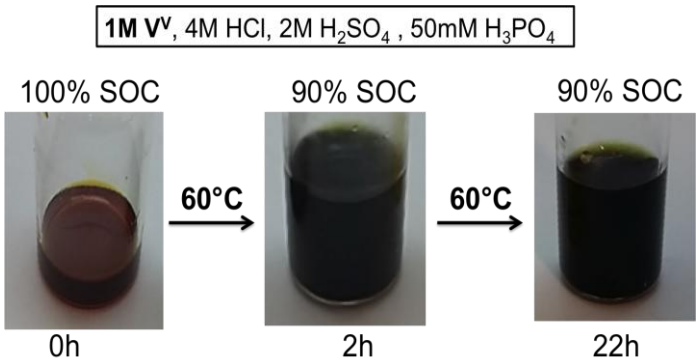

Figure S5: *thermal behavior of mixed–acid electrolyte with 1 M V^V at 60 °C.*

Figure S5 shows the evolution of the positive *mixed-acid electrolyte* at 60 °C. Initially the solution was dark brown, but it changed completely color after 2 hours. Moreover, a distinct smell of chlorine was noticed in the vial which was produced according to equation 13 of the main text. The state of charge, that it the ratio between V^V and V^{IV}, decreased to 90 % with the temperature. This was assured by potentiometric tests. However, the solution did not change for the next 20 hours, showing that it already reached equilibrium.
At the end of the tests, we also decided to decrease the maximal state of charge for the battery to 85 % in addition to the maximal total concentration of vanadium. This would both decrease the chance of formation of vanadium pentoxide in the *commercial electrolyte* and of chlorine evolution in the *mixed-acid electrolyte*.

C. Arrhenius study of vanadium redox couples

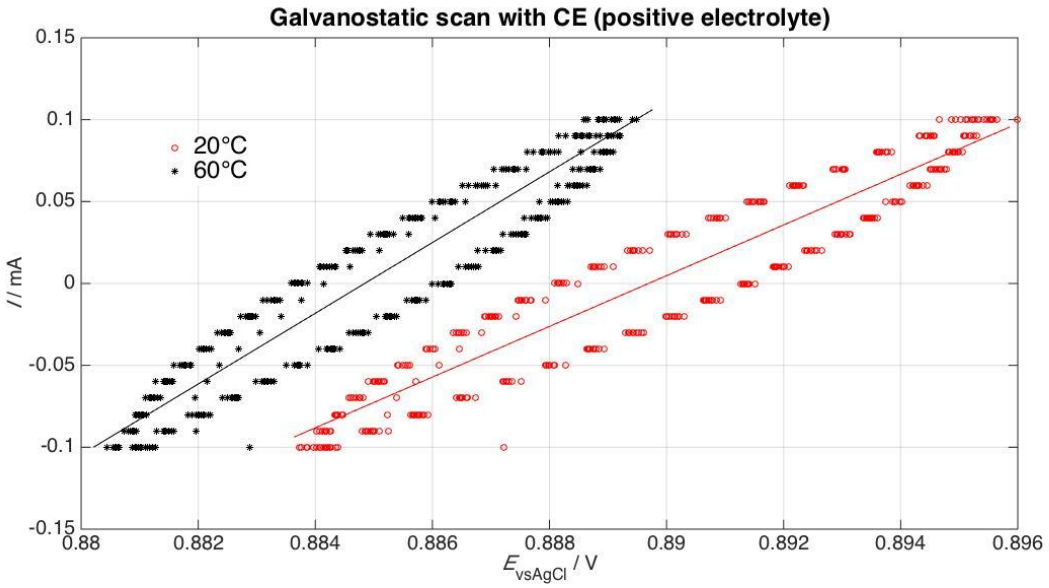

Figure S5: *Example of a galvanodynamic scan with the commercial electrolyte on the positive electrolyte at 20°C and 60°C.*

The temperature does not affect only the equilibrium potential of a reaction, but also its kinetics. Figure S4 shows some examples of the galvanodynamic cycle used to recover the equilibrium potential and the kinetic parameter (charge transfer resistance) at different temperatures. From the figure, it is clear that the potential shifted negatively and that the kinetics increased.
Assuming that the reaction follows an Arrhenius law:

$$\left(\quad \right) \quad — \qquad \text{(S1)}$$

Where k is the reaction constant, A the pre-exponential term, E_a the activation energy and R and T have the usual meaning. Rearranging equation S1:

$$\left(\quad \right) \quad — – \qquad \text{(S2)}$$

it is possible to recover the activation energy of the reaction from a simple linear regression. Note that instead of k equations S1 and S2 can be rewritten in function of the exchange current density or of the inverse of the charge transfer resistance, as it was done for this work.
The results are summarized in Table S1. It appeared that the behavior of V^{III}/V^{II} in the *commercial electrolyte* was atypical. In fact, the charge transfer resistance increased with temperature, therefore the activation energy for this reaction was not estimated. This was probably due to the fouling of the electrode surface, but it was not studied in details.

Table S1: *Activation energy, Ea, for positive and negative reaction with commercial and mixed-acid electrolyte.*

	E_a V^{III} / V^{II} / kJ·mol^{-1}	E_a V^{V} / V^{IV} / kJ·mol^{-1}

Commercial Electrolyte	–	7.3 ± 0.5
Mixed-Acid Electrolyte	37 ± 1	2.4 ± 0.6

From the data collected it is evident that the reaction was one order of magnitude faster for the positive electrolyte than for the negative one and the addition of chlorides in solution boost the positive reaction.

D. Photovoltaic and TREC-VRFB combination

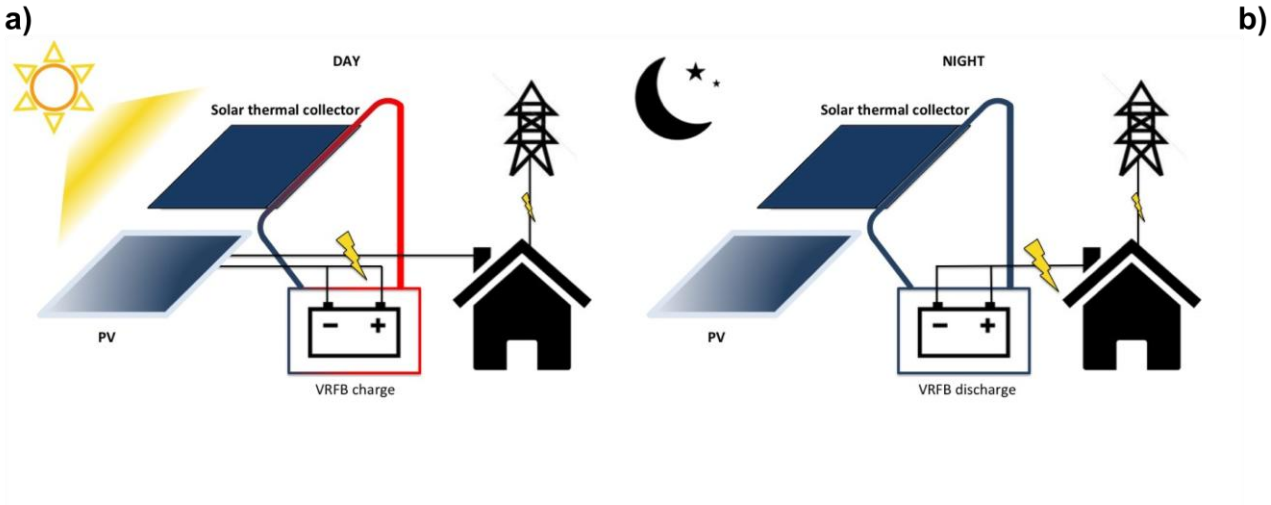

Figure S6: *schematic representation of a VRFB-TREC system coupled with photovoltaic and solar thermal collector. (**a**) During daylight, electricity and heat are available from sun irradiation for the charging cycle of the VRFB-TREC. (**b**) During the night when electricity is needed the battery can be discharged at a colder temperature closing the TREC cycle.*

Figure S6 illustrates the integration of a VRFB-TREC system with a photovoltaic (PV) and solar thermal collector.
During the day, the PV would produce electrical energy which, if in excess, can be stored in the VRFB. Ideally at this time both the PV and the solar thermal collector have a high temperature which can be used for the TREC, thus, enhancing the performances of the VRFB.
During the night, the process can be inverted and VRFB would be discharged to offset the absence of solar electrical resources. The PV and the solar thermal collector can be used as heat sink and provide the cold temperature for the TREC.
The advantage of such a system is in harvesting not only the portion of sun light which can be efficiently converted into electricity, but also all the infrared spectrum as heat. This heat, through the TREC enhances the performances of the VRFB.